
Towards Personalized Federated Learning via Heterogeneous Model Reassembly

Jiaqi Wang¹ Xingyi Yang² Suhan Cui¹ Liwei Che¹
Lingjuan Lyu³ Dongkuan Xu⁴ Fenglong Ma^{1*}

¹The Pennsylvania State University ²National University of Singapore

³Sony AI ⁴North Carolina State University

{jqwang, sxc6192, lfc5481, fenglong}@psu.edu,
xyang@u.nus.edu, lingjuan.lv@sony.com, dxu27@ncsu.edu

Abstract

This paper focuses on addressing the practical yet challenging problem of model heterogeneity in federated learning, where clients possess models with different network structures. To track this problem, we propose a novel framework called pFedHR, which leverages heterogeneous model reassembly to achieve personalized federated learning. In particular, we approach the problem of heterogeneous model personalization as a model-matching optimization task on the server side. Moreover, pFedHR automatically and dynamically generates informative and diverse personalized candidates with minimal human intervention. Furthermore, our proposed heterogeneous model reassembly technique mitigates the adverse impact introduced by using public data with different distributions from the client data to a certain extent. Experimental results demonstrate that pFedHR outperforms baselines on three datasets under both IID and Non-IID settings. Additionally, pFedHR effectively reduces the adverse impact of using different public data and dynamically generates diverse personalized models in an automated manner².

1 Introduction

Federated learning (FL) aims to enable collaborative machine learning without the need to share clients' data with others, thereby upholding data privacy [1, 2, 3]. However, traditional federated learning approaches [2, 4, 5, 6, 7, 8, 9, 10, 11, 12, 13, 14, 15] typically enforce the use of an identical model structure for all clients during training. This constraint poses challenges in achieving personalized learning within the FL framework. In real-world scenarios, clients such as data centers, institutes, or companies often possess their own distinct models, which may have varying structures. Training on top of their original models should be a better solution than deploying new ones for collaborative purposes. Therefore, a practical solution lies in fostering **heterogeneous model cooperation** within FL, while preserving individual model structures. Only a few studies have attempted to address the challenging problem of heterogeneous model cooperation in FL [16, 17, 18, 19, 20], and most of them incorporate the use of a public dataset to facilitate both cooperation and personalization [17, 18, 19, 20]. However, these approaches still face several key issues:

- **Undermining personalization through consensus:** Existing methods often generate consensual side information, such as class information [17], logits [18, 21], and label-wise representations [22], using public data. This information is then exchanged and used to conduct average operations on the server, resulting in a consensus representation. However, this approach poses privacy and

*Corresponding author.

²Source code can be found in the link <https://github.com/JackqqWang/pfedhr>

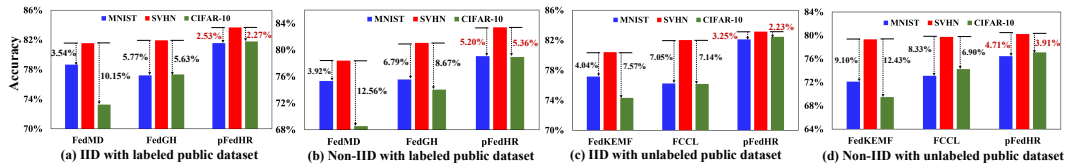


Figure 1: Performance changes when using different public data. pFedHR is our proposed model.

security concerns due to the exchange of side information [23]. Furthermore, the averaging process significantly diminishes the unique characteristics of individual local models, thereby hampering model personalization. Consequently, there is a need to explore approaches that can achieve local model personalization without relying on consensus-based techniques.

- Excessive reliance on prior knowledge for distillation-based approaches:** Distillation-based techniques, such as knowledge distillation (KD), are commonly employed for heterogeneous model aggregation in FL [19, 20, 24]. However, these techniques necessitate the predefinition of a shared model structure based on prior knowledge [20]. This shared model is then downloaded to clients to guide their training process. Consequently, handcrafted models can heavily influence local model personalization. Additionally, a fixed shared model structure may be insufficient for effectively guiding personalized learning when dealing with a large number of clients with non-IID data. Thus, it is crucial to explore methods that can automatically and dynamically generate client-specific personalized models as guidance.
- Sensitivity to the choice of public datasets:** Most existing approaches use public data to obtain guidance information, such as logits [18, 21] or a shared model [20], for local model personalization. The design of these approaches makes public data and model personalization **tightly bound together**. Thus, they usually choose the public data with the same distribution as the client data. Therefore, using public data with different distributions from client data will cause a significant performance drop in existing models. Figure 1 illustrates the performance variations of different models trained on the SVHN dataset with different public datasets (detailed experimental information can be found in Section 4.4). The figure demonstrates a significant performance drop when using alternative public datasets. Consequently, mitigating the adverse impact of employing diverse public data remains a critical yet practical research challenge in FL.

Motivation & Challenges. In fact, both consensus-based and distillation-based approaches aim to learn aggregated and shared information used as guidance in personalized local model training, which is not an optimal way to achieve personalization. An ideal solution is to generate a personalized model for the corresponding client, which is significantly challenging since the assessable information on the server side can only include the uploaded client models and the public data. To avoid the issue of public data sensitivity, only client models can be used. These constraints motivate us to employ the model reassembly technique [25] to generate models first and then select the most matchable personalized model for a specific client from the generations.

To this end, we will face several new challenges. **(C1)** Applying the model reassembly technique will result in many candidates. Thus, the first challenge is how to get the optimal candidates. **(C2)** The layers of the generated candidates are usually from different client models, and the output dimension size of the first layer may not align with the input dimension size of the second layer, which leads to the necessity of network layer stitching. However, the parameters of the stitched layers are unknown. Therefore, the second challenge is how to learn those unknown parameters in the stitched models. **(C3)** Even with well-trained stitched models, digging out the best match between a client model and a stitched model remains a big challenge.

Our Approach. To simultaneously tackle all the aforementioned challenges, we present a novel framework called pFedHR, which aims to achieve personalized federated learning and address the issue of heterogeneous model cooperation (as depicted in Figure 2). The pFedHR framework comprises two key updates: the server update and the client update. In particular, to tackle **C3**, we approach the issue of heterogeneous model personalization from a model-matching optimization perspective on the **server** side (see Section 3.1.1). To solve this problem, we introduce a novel **heterogeneous model reassembly** technique in Section 3.1.2 to assemble models uploaded from clients, i.e., $\{\mathbf{w}_t^1, \dots, \mathbf{w}_t^B\}$, where B is the number of active clients in the t -th communication round. This technique involves the dynamic grouping of model layers based on their functions, i.e., *layer-wise decomposition* and *function-driven layer grouping* in Figure 2. To handle **C1**, a heuristic

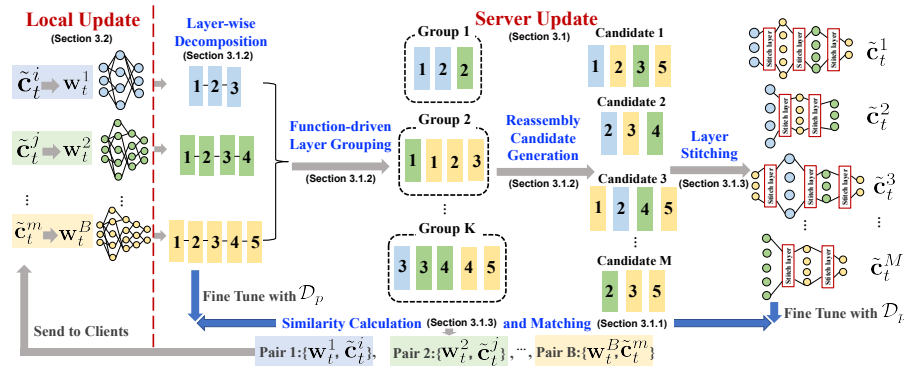


Figure 2: Overview of the proposed pFedHR. K is the number of clusters.

rule-based search strategy is proposed in *reassembly candidate generation* to assemble informative and diverse model candidates using clustering results. Importantly, all layers in each candidate are derived from the uploaded client models.

Prior to matching the client model with candidates, we perform network *layer stitching* while maximizing the retention of information from the original client models (Section 3.1.3). To tackle **C2**, we introduce public data \mathcal{D}_p to help the finetuning of the stitched candidates, i.e., $\{\tilde{c}_t^1, \dots, \tilde{c}_t^M\}$, where M is the number of generated candidates. Specifically, we employ labeled **OR** unlabeled public data to fine-tune the stitched and client models and then calculate similarities based on model outputs. Intuitively, if two models are highly related to each other, their outputs should also be similar. Therefore, we select the candidate with the highest similarity as the personalized model of the corresponding client, which results in matched pairs $\{\{w_t^1, \tilde{c}_t^1\}, \dots, \{w_t^B, \tilde{c}_t^B\}\}$ in Figure 2. In the **client** update (Section 3.2), we treat the matched personalized model as a guidance mechanism for client parameter learning using knowledge distillation³.

It is worth noting that we **minimally use public data** during our model learning to reduce their adverse impact. In our model design, the public data are used for clustering layers, fine-tuning the stitched candidates, and guiding model matching. Clustering and matching stages use public data to obtain the feedforward outputs as guidance and do not involve model parameter updates. *Only in the fine-tuning stage, the stitched models' parameters will be updated based on public data.* To reduce its impact as much as possible, we limit the number of finetuning epochs during the model implementation. Although we cannot thoroughly break the tie between model training and public data, such a design at least greatly alleviates the problem of public data sensitivity in FL.

Contributions. Our work makes the following key contributions: (1) We introduce the first personalized federated learning framework based on model reassembly, specifically designed to address the challenges of heterogeneous model cooperation. (2) The proposed pFedHR framework demonstrates the ability to automatically and dynamically generate personalized candidates that are both informative and diverse, requiring minimal human intervention. (3) We present a novel heterogeneous model reassembly technique, which effectively mitigates the adverse impact caused by using public data with distributions different from client data. (4) Experimental results show that the pFedHR framework achieves state-of-the-art performance on three datasets, exhibiting superior performance under both IID and Non-IID settings when compared to baselines employing labeled and unlabeled public datasets.

2 Related Work

Model Heterogeneity in Federated Learning. Although many federated learning models, such as FedAvg [4], FedProx [2], Per-FedAvg [26], PFedMe [27], and PFedBayes[28], have been proposed recently, the focus on heterogeneous model cooperation, where clients possess models with diverse structures, remains limited. It is worth noting that in this context, the client models are originally distinct and not derived from a shared, large global model through the distillation of subnetworks [29, 30]. Existing studies on heterogeneous model cooperation can be broadly categorized based on whether they utilize public data for model training. FedKD [16] aims to achieve personalized models

³Note that the network architecture of both local model and personalized model are known, and thus, there is no human intervention in the client update.

Table 1: A comparison between existing heterogeneous model cooperation works and our pFedHR.

Approach	Public Dataset		Model Characteristics		
	W. Label	W.o. Label	Upload and Download	Aggregation	Personalization
FedDF [19]	✗	✓	parameters	ensemble distillation	✗
FedKEMF [20]	✗	✓	parameters	mutual learning	✓
FCCL [18]	✗	✓	logits	average	✓
FedMD [17]	✓	✗	class scores	average	✓
FedGH [22]	✓	✗	label-wise representations	average	✓
pFedHR	✓	✓	parameters	model reassembly	✓

for each client **without employing public data** by simultaneously maintaining a large heterogeneous model and a small homogeneous model on each client, which incurs high computational costs.

Most existing approaches **leverage public data** to facilitate model training. Among them, FedDF [19], FedKEMF [20], and FCCL [18] employ *unlabeled public data*. However, FedDF trains a global model with different settings compared to our approach. FedKEMF performs mutual knowledge distillation learning on the server side to achieve model personalization, requiring predefined model structures. FCCL averages the logits provided by each client and utilizes a consensus logit as guidance during local model training. It is worth noting that the use of logits raises concerns regarding privacy and security [23, 31]. FedMD [17] and FedGH [22] employ *labeled public data*. These approaches exchange class information or representations between the server and clients and perform aggregation to address the model heterogeneity issue. However, similar to FCCL, these methods also introduce privacy leakage concerns. In contrast to existing work, we propose a general framework capable of utilizing either **labeled OR unlabeled public data** to learn personalized models through heterogeneous model reassembly. We summarize the distinctions between existing approaches and our framework in Table 1.

Neural Network Reassembly and Stitching. As illustrated in Table 1, conventional methods are primarily employed in existing federated learning approaches to obtain personalized client models, with limited exploration of model reassembly. Additionally, there is a lack of research investigating neural network reassembly and stitching [25, 32, 33, 34, 35, 36] within the context of federated learning. For instance, the work presented in [33] proposes three algorithms to merge two models within the weight space, but it is limited to handling only two models as input. In our setting, multiple models need to be incorporated into the model reassembly or aggregation process. Furthermore, both [25] and [34] focus on pre-trained models, which differ from our specific scenario.

3 Methodology

Our model pFedHR incorporates two key updates: the server update and the local update, as depicted in Figure 2. Next, we provide the details of our model design starting with the server update.

3.1 Server Update

During each communication round t , the server will receive B heterogeneous client models with parameters denoted as $\{\mathbf{w}_t^1, \mathbf{w}_t^2, \dots, \mathbf{w}_t^B\}$. As we discussed in Section 1, traditional approaches have limitations when applied in this context. To overcome these limitations and learn a personalized model $\hat{\mathbf{w}}_t^n$ that can be distributed to the corresponding n -th client, we propose a novel approach that leverages the publicly available data \mathcal{D}_p stored on the server to find the **most similar** aggregated models learned from $\{\mathbf{w}_t^1, \mathbf{w}_t^2, \dots, \mathbf{w}_t^B\}$ for \mathbf{w}_t^n .

3.1.1 Similarity-based Model Matching

Let $g(\cdot, \cdot)$ denote the model aggregation function, which can automatically and dynamically obtain M aggregated model candidates as follows:

$$\{\mathbf{c}_t^1, \dots, \mathbf{c}_t^M\} = g(\{\mathbf{w}_t^1, \mathbf{w}_t^2, \dots, \mathbf{w}_t^B\}, \mathcal{D}_p), \quad (1)$$

where $g(\cdot, \cdot)$ will be detailed in Section 3.1.2, and \mathbf{c}_k^m is the m -th generated model candidate learned by $g(\cdot, \cdot)$. Note that \mathbf{c}_k^m denotes the model before network stitching. M is the total number of candidates, which is not a fixed number and is estimated by $g(\cdot, \cdot)$. In such a way, our goal is to optimize the following function:

$$\mathbf{c}_t^* = \arg \max_{\mathbf{c}_t^m; m \in [1, M]} \{\text{sim}(\mathbf{w}_t^n, \mathbf{c}_t^1; \mathcal{D}_p), \dots, \text{sim}(\mathbf{w}_t^n, \mathbf{c}_t^M; \mathcal{D}_p)\}, \forall n \in [1, B], \quad (2)$$

Algorithm 1: Reassembly Candidate Search

input : Layer clusters $\{\mathcal{G}_t^1, \mathcal{G}_t^2, \dots, \mathcal{G}_t^K\}$, operation type set \mathcal{O} , rule set \mathcal{R}
output : $\{\mathbf{c}_t^1, \dots, \mathbf{c}_t^M\}$

- 1 Initialize $\mathcal{C}_t = \emptyset$;
- 2 **for** $k \leftarrow 1, \dots, K$ **do**
- 3 // Q_k is the number of operation-layer pairs in \mathcal{G}_t^k
- 4 **for** $q \leftarrow 1, \dots, Q_k$ **do**
- 5 Initialize an empty candidate $\mathbf{c}_q = []$, operation type set $\mathcal{O}_q = \emptyset$, group id set $\mathcal{K}_q = \emptyset$;
- 6 Select the q -th layer-operation pair $(\mathcal{L}_{t,i}^n, O_i^n)$ from group \mathcal{G}_t^k
- 7 Add $(\mathcal{L}_{t,i}^n, O_i^n)$ to \mathbf{c}_q , add O_i^n to \mathcal{O}_q , add k to \mathcal{K}_q ;
- 8 **for** $k' \leftarrow 1, \dots, K$ **do**
- 9 Check a pair from $\mathcal{G}_{k'}$ whether it satisfies:
- 10 \mathcal{R}_1 (layer order): the layer index should be larger than that of the last layer added to \mathbf{c}_q ,
 and
- 11 \mathcal{R}_2 (operation order): the operation type should be followed by the previous type in \mathbf{c}_q ;
- 12 **if True then**
- 13 Add the pair to \mathbf{c}_q , add its operation type to \mathcal{O}_q , add k' to \mathcal{K}_q ;
- 14 Move to the next pair;
- 15 Check \mathcal{O}_q and \mathcal{K}_q with:
- 16 \mathcal{R}_3 (complete operation): the size of \mathcal{O}_q should be equal to that of \mathcal{O} , and
- 17 \mathcal{R}_4 (diverse group): the size of \mathcal{K}_q should be equal to K ;
- 18 **if True then**
- 19 Add the candidate \mathbf{c}_q to \mathcal{C}_t ;

return : $\mathcal{C}_t = \{\mathbf{c}_t^1, \dots, \mathbf{c}_t^M\}$

where \mathbf{c}_t^* is the best matched model for \mathbf{w}_t^n , which is also denoted as $\hat{\mathbf{w}}_t^n = \mathbf{c}_t^*$. $\text{sim}(\cdot, \cdot)$ is the similarity function between two models, which will be detailed in Section 3.1.3.

3.1.2 Heterogeneous Model Reassembly – $g(\cdot, \cdot)$

To optimize Eq. (2), we need to obtain M candidates using the heterogenous model aggregation function $g(\cdot)$ in Eq. (1). To avoid the issue of predefined model architectures in the knowledge distillation approaches, we aim to automatically and dynamically learn the candidate architectures via a newly designed function $g(\cdot, \cdot)$. In particular, we propose a decomposition-grouping-reassembly method as $g(\cdot, \cdot)$, including layer-wise decomposition, function-driven layer grouping, and reassembly candidate generation.

Layer-wise Decomposition. Assume that each uploaded client model \mathbf{w}_t^n contains H layers, i.e., $\mathbf{w}_t^n = [(\mathbf{L}_{t,1}^n, O_1^n), \dots, (\mathbf{L}_{t,H}^n, O_H^n)]$, where each layer $\mathbf{L}_{t,h}^n$ is associated with an operation type O_h^n . For example, a plain convolutional neural network (CNN) usually has three operations: convolution, pooling, and fully connected layers. For different client models, H may be different. The decomposition step aims to obtain these layers and their corresponding operation types.

Function-driven Layer Grouping. After decomposing layers of client models, we group these layers based on their functional similarities. Due to the model structure heterogeneity in our setting, the dimension size of the output representations from layers by feeding the public data \mathcal{D}_p to different models will be different. Thus, measuring the similarity between a pair of layers is challenging, which can be resolved by applying the commonly used centered kernel alignment (CKA) technique [37]. In particular, we define the distance metric between any pair of layers as follows:

$$\text{dis}(\mathbf{L}_{t,i}^n, \mathbf{L}_{t,j}^b) = (\text{CKA}(\mathbf{X}_{t,i}^n, \mathbf{X}_{t,j}^b) + \text{CKA}(\mathbf{L}_{t,i}^n(\mathbf{X}_{t,i}^n), \mathbf{L}_{t,i}^b(\mathbf{X}_{t,j}^b)))^{-1}, \quad (3)$$

where $\mathbf{X}_{t,i}^n$ is the input data of $\mathbf{L}_{t,i}^n$, and $\mathbf{L}_{t,i}^n(\mathbf{X}_{t,i}^n)$ denotes the output data from $\mathbf{L}_{t,i}^n$. This metric uses $\text{CKA}(\cdot, \cdot)$ to calculate the similarity between both input and output data of two layers.

Based on the defined distance metric, we conduct the K-means-style algorithm to group the layers of B models into K clusters. This optimization process aims to minimize the sum of distances between

all pairs of layers, denoted as \mathcal{L}_t . The procedure can be described as follows:

$$\min \mathcal{L}_t = \min_{\delta_{b,h}^a \in \{0,1\}} \sum_{k=1}^K \sum_{b=1}^B \sum_{h=1}^H \delta_{b,h}^k (\text{dis}(\mathbf{L}_t^k, \mathbf{L}_{t,h}^b)), \quad (4)$$

where \mathbf{L}_t^k is the center of the k -th cluster. $\delta_{b,h}^k$ is the indicator. If the h -th layer of \mathbf{w}_t^b belongs to the k -th cluster, then $\delta_{b,h}^k = 1$. Otherwise, $\delta_{b,h}^k = 0$. After the grouping process, we obtain K layer clusters denoted as $\{\mathcal{G}_t^1, \mathcal{G}_t^2, \dots, \mathcal{G}_t^K\}$. There are multiple layers in each group, which have similar functions. Besides, each layer is associated with an operation type.

Reassembly Candidate Generation. The last step for obtaining personalized candidates $\{\mathbf{c}_t^1, \dots, \mathbf{c}_t^M\}$ is to assemble the learned layer-wise groups $\{\mathcal{G}_t^1, \mathcal{G}_t^2, \dots, \mathcal{G}_t^K\}$ based on their functions. To this end, we design a heuristic rule-based search strategy as shown in Algorithm 1. Our goal is to automatically generate *informative* and *diverse* candidates.

Generally, an **informative** candidate needs to follow the design of handcrafted network structures. This is challenging since the candidates are automatically generated without human interventions and prior knowledge. To satisfy this condition, we require the layer orders to be guaranteed (\mathcal{R}_1 in Line 10). For example, the i -th layer from the n -th model, i.e., $\mathbf{L}_{t,i}^n$, in a candidate must be followed by a layer with an index $j > i$ from other models or itself. Besides, the operation type also determines the quality of a model. For a CNN model, the fully connected layer is usually used after the convolution layer, which motivates us to design the \mathcal{R}_2 operation order rule in Line 11.

Only taking the informativeness principle into consideration, we may generate a vast number of candidates with different sizes of layers. Some candidates may be a subset of others and even worse with low quality. Besides, the large number of candidates will increase the computational burden of the server. To avoid these issues and further obtain high-quality candidates, we use the **diversity** principle as the filtering rule. A diverse and informative model should contain all the operation types, i.e., the \mathcal{R}_3 complete operation rule in Line 16. Besides, the groups $\{\mathcal{G}_t^1, \dots, \mathcal{G}_t^K\}$ are clustered based on their layer functions. The requirement that layers of candidates must be from different groups should significantly increase the diversity of model functions, which motivates us to design the \mathcal{R}_4 diverse group rule in Line 17.

3.1.3 Similarity Learning with Layer Stitching – $\text{sim}(\cdot, \cdot)$

After obtaining a set of candidate models $\{\mathbf{c}_t^1, \dots, \mathbf{c}_t^M\}$, to optimize Eq. (2), we need to calculate the similarity between each client model \mathbf{w}_t^n and all the candidates $\{\mathbf{c}_t^1, \dots, \mathbf{c}_t^M\}$ using the public data \mathcal{D}_p . However, this is non-trivial since \mathbf{c}_t^m is assembled by layers from different client models, which is not a complete model architecture. We have to stitch these layers together before using \mathbf{c}_t^m .

Layer Stitching. Assume that $\mathbf{L}_{t,i}^n$ and $\mathbf{L}_{t,j}^b$ are any two consecutive layers in the candidate model \mathbf{c}_t^m . Let d_i denote the output dimension of $\mathbf{L}_{t,i}^n$ and d_j denote the input dimension of $\mathbf{L}_{t,j}^b$. d_i is usually not equal to d_j . To stitch these two layers, we follow existing work [34] by adding a nonlinear activation function $\text{ReLU}(\cdot)$ on top of a linear layer, i.e., $\text{ReLU}(\mathbf{W}^\top \mathbf{X} + \mathbf{b})$, where $\mathbf{W} \in \mathbb{R}^{d_i \times d_j}$, $\mathbf{b} \in \mathbb{R}^{d_j}$, and \mathbf{X} represents the output data from the first layer. In such a way, we can obtain a stitched candidate $\tilde{\mathbf{c}}_t^m$. The reasons that we apply this simple layer as the stitch are twofold. On the one hand, even adding a simple linear layer between any two consecutive layers, the model will increase $d_i * (d_j + 1)$ parameters. Since a candidate \mathbf{c}_t^m may contain several layers, if using more complicated layers as the stitch, the number of parameters will significantly increase, which makes the new candidate model hard to be trained. On the other hand, using a simple layer with a few parameters may be helpful for the new candidate model to maintain more information from the original models. This is of importance for the similarity calculation in the next step.

Similarity Calculation. We propose to use the cosine score $\text{cos}(\cdot, \cdot)$ to calculate the similarity between a pair of models $(\mathbf{w}_t^n, \tilde{\mathbf{c}}_t^m)$ as follows:

$$\text{sim}(\mathbf{w}_t^n, \mathbf{c}_t^m; \mathcal{D}_p) = \text{sim}(\mathbf{w}_t^n, \tilde{\mathbf{c}}_t^m; \mathcal{D}_p) = \frac{1}{P} \sum_{p=1}^P \text{cos}(\boldsymbol{\alpha}_t^n(\mathbf{x}_p), \boldsymbol{\alpha}_t^m(\mathbf{x}_p)), \quad (5)$$

where P denotes the number of data in the public dataset \mathcal{D}_p and \mathbf{x}_p is the p -th data in \mathcal{D}_p . $\boldsymbol{\alpha}_t^n(\mathbf{x}_p)$ and $\boldsymbol{\alpha}_t^m(\mathbf{x}_p)$ are the logits output from models \mathbf{w}_t^n and $\tilde{\mathbf{c}}_t^m$, respectively. To obtain the logits, we

need to finetune \mathbf{w}_t^n and $\tilde{\mathbf{c}}_t^m$ using \mathcal{D}_p first. In our design, we can use both labeled and unlabeled data to finetune models but with different loss functions. If \mathcal{D}_p is **labeled**, then we use the supervised cross-entropy (CE) loss to finetune the model. If \mathcal{D}_p is **unlabeled**, then we apply the self-supervised contrastive loss to finetune them following [38].

3.2 Client Update

The obtained personalized model $\hat{\mathbf{w}}_t^n$ (i.e., \mathbf{c}_t^* in Eq. (2)) will be distributed to the n -th client if it is selected in the next communication round $t + 1$. $\hat{\mathbf{w}}_t^n$ is a reassembled model that carries external knowledge from other clients, but its network structure is different from the original \mathbf{w}_t^n . To incorporate the new knowledge without training \mathbf{w}_t^n from scratch, we propose to apply knowledge distillation on the client following [39].

Let $\mathcal{D}_n = \{(\mathbf{x}_i^n, \mathbf{y}_i^n)\}$ denote the labeled data, where \mathbf{x}_i^n is the data feature and \mathbf{y}_i^n is the corresponding ground truth vector. The loss of training local model with knowledge distillation is defined as follows:

$$\mathcal{J}_n = \frac{1}{|\mathcal{D}_n|} \sum_{i=1}^{|\mathcal{D}_n|} [\text{CE}(\mathbf{w}_t^n(\mathbf{x}_i^n), \mathbf{y}_i^n) + \lambda \text{KL}(\boldsymbol{\alpha}_t^n(\mathbf{x}_i^n), \hat{\boldsymbol{\alpha}}_t^n(\mathbf{x}_i^n))], \quad (6)$$

where $|\mathcal{D}_n|$ denotes the number of data in \mathcal{D}_n , $\mathbf{w}_t^n(\mathbf{x}_i^n)$ means the predicted label distribution, λ is a hyperparameter, $\text{KL}(\cdot, \cdot)$ is the Kullback–Leibler divergence, and $\boldsymbol{\alpha}_t^n(\mathbf{x}_i^n)$ and $\hat{\boldsymbol{\alpha}}_t^n(\mathbf{x}_i^n)$ are the logits from the local model \mathbf{w}_t^n and the downloaded personalized model $\hat{\mathbf{w}}_t^n$, respectively.

4 Experiments

4.1 Experiment Setups

Datasets. We conduct experiments for the image classification task on MNIST, SVHN, and CIFAR-10 datasets under both IID and non-IID data distribution settings, respectively. We split the datasets into 80% for training and 20% for testing. During training, we randomly sample 10% training data to put in the server as \mathcal{D}_p and the remaining 90% to distribute to the clients. The training and testing datasets are randomly sampled for the IID setting. For the non-IID setting, each client randomly holds two classes of data. To test the personalization effectiveness, we sample the testing dataset following the label distribution as the training dataset. We also conduct experiments to test models using **different public data** in Section 4.4.

Baselines. We compare pFedHR with the baselines under two settings. (1) **Heterogenous setting.** In this setting, clients are allowed to have different model structures. The proposed pFedHR is general and can use both labeled and unlabeled public datasets to conduct heterogeneous model cooperation. To make fair comparisons, we use FedMD [17] and FedGH [22] as baselines when using the *labeled public data*, and FCCL [18] and FedKEMF [20] when testing the *unlabeled public data*. (2) **Homogenous setting.** In this setting, clients share an identical model structure. We use traditional and personalized FL models as baselines, including FedAvg [4], FedProx [2], Per-FedAvg [26], PFedMe [27], and PFedBayes [28].

4.2 Heterogenous Setting Evaluation

Small Number of Clients. Similar to existing work [18], to test the performance with a small number of clients, we set the client number $N = 12$ and active client number $B = 4$ in each communication round. We design 4 types of models with different structures and randomly assign each type of model to 3 clients. The *Conv* operation contains convolution, max pooling, batch normalization, and ReLU, and the *FC* layer contains fully connected mapping, ReLU, and dropout. We set the number of clusters $K = 4$. Then local training epoch and the server finetuning epoch are equal to 10 and 3, respectively. The public data and client data are from the same dataset.

Table 2 shows the experimental results for the heterogeneous setting using both labeled and unlabeled public data. We can observe that the proposed pFedHR achieves state-of-the-art performance on all datasets and settings. We also find the methods using labeled public datasets can boost the performance compared with unlabeled public ones in general, which aligns with our expectations and experiences.

Table 2: Performance comparison with baselines under the heterogeneous setting.

Public Data	Dataset	MNIST		SVHN		CIFAR-10	
	Model	IID	Non-IID	IID	Non-IID	IID	Non-IID
Labeled	FedMD [17]	93.08%	91.44%	81.55%	78.39%	68.22%	66.13%
	FedGH [22]	94.10%	93.27%	81.94%	81.06%	72.69%	70.27%
	pFedHR	94.55%	94.41%	83.68%	83.40%	73.88%	71.74%
Unlabeled	FedKEMF [20]	93.01%	91.66%	80.41%	79.33%	67.12%	66.93%
	FCCL [18]	93.62%	92.88%	82.03%	79.75%	68.77%	66.49%
	pFedHR	93.89%	93.76%	83.15%	80.24%	69.38%	68.01%

Large Number of Clients. We also test the performance of models with a large number of clients. When the number of active clients B is large, calculating layer pair-wise distance values using Eq. (3) will be highly time-consuming. To avoid this issue, a straightforward solution is to conduct FedAvg [4] for averaging the models with the same structures first and then do the function-driven layer grouping based on the averaged structures via Eq. (4). The following operations are the same as pFedHR. In this experiment, we set $N = 100$ clients and the active number of clients $B = 10$. Other settings are the same as those in the small number client experiment.

Table 3 shows the results on the SVHN dataset for testing the proposed pFedHR for a large number of clients setting. The results show similar patterns as those listed in Table 2, where the proposed pFedHR achieves the best performance under IID and Non-IID settings whether it uses labeled or unlabeled public datasets. Compared to the results on the SVHN dataset in Table 2, we can find that the performance of all the baselines and our models drops. Because the number of training data is fixed, allocating these data to 100 clients will make each client use fewer data for training, which leads to a performance drop. The results on both small and large numbers of clients clearly demonstrate the effectiveness of our model for addressing the heterogeneous model cooperation issue in federated learning.

Table 3: Evaluation using a large number of clients on the SVHN dataset ($N = 100$).

Public Data	Model	IID	Non-IID
Labeled	FedMD	78.16%	74.34%
	FedGH	76.27%	72.78%
	pFedHR	80.02%	77.63%
Unlabeled	FedKEAF	76.27%	74.61%
	FCCL	75.03%	71.54%
	pFedHR	78.98%	75.77%

4.3 Homogeneous Setting Evaluation

In this experiment, all the clients use the same model structure. We test the performance of our proposed pFedHR on representative models with the smallest (M1) and largest (M4) number of layers, compared with state-of-the-art homogeneous federated learning models. Except for the identical model structure, other experimental settings are the same as those used in the scenario of the small number of clients. Note that for pFedHR, we report the results using the labeled public data in this experiment. The results are shown in Table 4.

Table 4: Homogeneous model comparison with baselines.

Model	Dataset	MNIST		SVHN		CIFAR-10	
	Setting	IID	Non-IID	IID	Non-IID	IID	Non-IID
M1	FedAvg [4]	91.23%	90.04%	53.45%	51.33%	43.05%	33.39%
	FedProx [2]	92.66%	92.47%	54.86%	53.09%	43.62%	35.06%
	Per-FedAvg [26]	93.23%	93.04%	54.29%	52.04%	44.14%	42.02%
	PFedMe [27]	93.57%	92.00%	55.01%	53.78%	45.01%	43.65%
	PFedBayes [28]	94.39%	93.32%	58.49%	55.74%	46.12%	44.49%
	pFedHR	94.26%	93.26%	61.72%	59.23%	54.38%	48.44%
M4	FedAvg [4]	94.24%	92.16%	83.26%	82.77%	67.68%	58.92%
	FedProx [2]	94.22%	93.22%	84.72%	83.00%	71.24%	63.98%
	Per-FedAvg [26]	95.77%	93.67%	85.99%	84.01%	79.56%	76.23%
	PFedMe [27]	95.71%	94.02%	87.63%	85.33%	79.88%	77.56%
	PFedBayes [28]	95.64%	93.23%	88.34%	86.28%	80.06%	77.93%
	pFedHR	94.88%	93.77%	89.87%	87.94%	81.54%	79.45%

We can observe that using a simple model (M1) can make models achieve relatively high performance since the MNIST dataset is easy. However, for complicated datasets, i.e., SVHN and CIFAR-10, using a complex model structure (i.e., M4) is helpful for all approaches to improve their performance significantly. Our proposed pFedHR outperforms all baselines on these two datasets, even equipping with a simple model M1. Note that our model is proposed to address the heterogeneous model cooperation problem instead of the homogeneous personalization in FL. Thus, it is a practical

approach and can achieve personalization. Still, we also need to mention that it needs extra public data on the server, which is different from baselines.

4.4 Public Dataset Analysis

Sensitivity to the Public Data Selection. In the previous experiments, the public and client data are from the same dataset, i.e., having the same distribution. To validate the effect of using different public data during model learning for all baselines and our model, we conduct experiments by choosing public data from different datasets and report the results on the SVHN dataset. Other experimental settings are the same as those in the scenario of the small number of clients.

Figure 1 shows the experimental results for all approaches using labeled and unlabeled public datasets. We can observe that replacing the public data will make all approaches decrease performance. This is reasonable since the data distributions between public and client data are different. However, compared with baselines, the proposed $pFedHR$ has the **lowest performance drop**. *Even using other public data, $pFedHR$ can achieve comparable or better performance with baselines using SVHN as the public data.* This advantage stems from our model design. As described in Section 3.1.3, we keep more information from original client models by using a simple layer as the stitch. Besides, we aim to search for the most similar personalized candidate with a client model. We propose to calculate the average logits in Eq. (5) as the criteria. To obtain the logits, we do not need to finetune the models many times. In our experiments, we set the number of finetuning epochs as 3. This strategy can also help the model reduce the adverse impact of public data during model training.

Sensitivity to the Percentage of Public Data. Several factors can affect model performance. In this experiment, we aim to investigate whether the percentage of public data is a key factor in influencing performance change. Toward this end, we still use the small number of clients setting, i.e., the client and public data are from the SVHN dataset, but we adjust the percentage of public data. In the original experiment, we used 10% data as the public data. Now, we reduce this percentage to 2% and 5%. The results are shown in Figure 3. We can observe that with the increase in the percentage of public data, the performance of the proposed $pFedHR$ also improves. These results align with our expectations since more public data used for finetuning can help $pFedHR$ obtain more accurately matched personalized models, further enhancing the final accuracy.

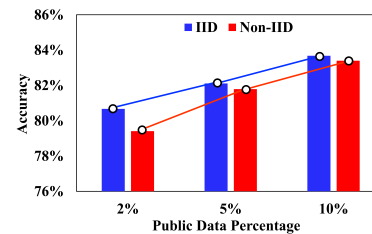


Figure 3: Performance change w.r.t. the percentage of public data.

4.5 Experiment results with Different Numbers of Clusters

In our model design, we need to group functional layers into K groups by optimizing Eq. (4). Where K is a predefined hyperparameter. In this experiment, we aim to investigate the performance influence with regard to K . In particular, we conduct the experiments on the SVHN dataset with 12 local clients, and the public data are also the SVHN data.

Figure 4 shows the results on both IID and Non-IID settings with labeled and unlabeled public data. X -axis represents the number of clusters, and Y -axis denotes the accuracy values. We can observe that with the increase of K , the performance will also increase. However, in the experiments, we do not recommend setting a large K since a trade-off balance exists between K and M , where M is the number of candidates automatically generated by Algorithm 1 in the main manuscript. If K is large, then M will be small due to Rule \mathcal{R}_4 . In other words, a larger K may make the empty \mathcal{C}_t returned by Algorithm 1 in the main manuscript.

4.6 Layer Stitching Study

One of our major contributions is to develop a new layer stitching strategy to reduce the adverse impacts of introducing public data, even with different distributions from the client data. Our proposed strategy includes two aspects: (1) using a simple layer to stitch layers and (2) reducing the number of finetuning epochs. To validate the correctness of these assumptions, we conduct the following experiments on SVHN with 12 clients, where both client data and **labeled** public data are extracted from SVHN.

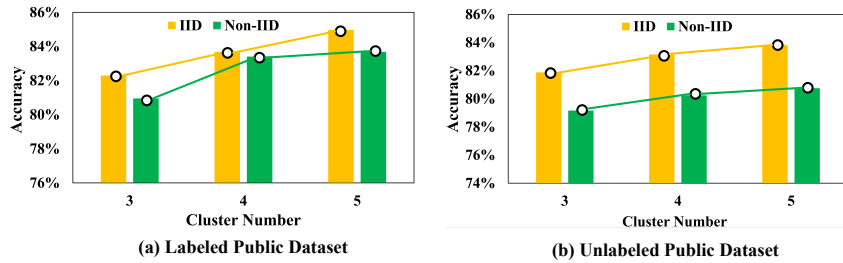


Figure 4: Results on different number of clusters K 's.

Stitching Layer Numbers. In this experiment, we add the complexity of layers for stitching. In our model design, we only use $\text{ReLU}(\mathbf{W}^T \mathbf{X} + \mathbf{b})$. Now, we increase the number of linear layers from 1 to 2 to 3. The results are depicted in Figure 5. We can observe that under both IID and Non-IID settings, the performance will decrease with the increase of the complexity of the stitching layers. These results demonstrate our assumption that more complex stitching layers will introduce more information about public data but reduce the personalized information of each client model maintained. Thus, using a simple layer to stitch layers is a reasonable choice.

Stitched Model Finetuning Numbers. We further explore the influence of the number of finetuning epochs on the stitched model. The results are shown in Figure 6. We can observe that increasing the number of finetuning epochs can also introduce more public data information and reduce model performance. Thus, setting a small number of finetuning epochs benefits keeping the model's performance.

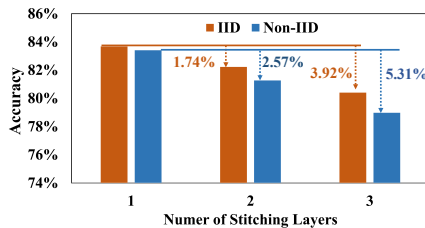


Figure 5: Stitching layer number study.

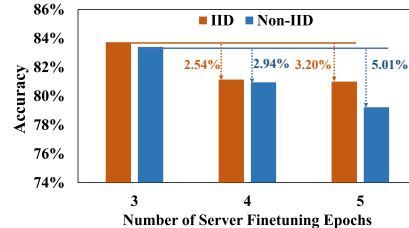


Figure 6: Server finetuning number study.

4.7 Personalized Model Visualization

pFedHR can automatically and dynamically generate candidates for clients using the proposed heterogeneous model reassembly techniques in Section 3.1.2. We visualize the generated models for a client at two different epochs (t and t') to make a comparison in Figure 7. We can observe that at epoch t , the layers are “[Conv2 from M1, Conv3 from M2, Conv4 from M3, Conv5 from M3, FC3 from M2]”, which is significantly different the model structure at epoch t' . These models automatically reassemble different layers from different models learned by the proposed pFedHR instead of using predefined structures or consensus information.

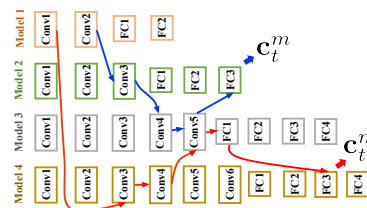


Figure 7: Candidate models.

5 Conclusion

Model heterogeneity is a crucial and practical challenge in federated learning. While a few studies have addressed this problem, existing models still encounter various issues. To bridge this research gap, we propose a novel framework, named pFedHR, for personalized federated learning, focusing on solving the problem of heterogeneous model cooperation. The experimental results conducted on three datasets, under both IID and Non-IID settings, have verified the effectiveness of our proposed pFedHR framework in addressing the model heterogeneity issue in federated learning. The achieved state-of-the-art performance serves as evidence of the efficacy and practicality of our approach.

Acknowledgements This work is partially supported by the National Science Foundation under Grant No. 2212323 and 2238275.

References

- [1] Peter Kairouz, H Brendan McMahan, Brendan Avent, Aurélien Bellet, Mehdi Bennis, Arjun Nitin Bhagoji, Kallista Bonawitz, Zachary Charles, Graham Cormode, Rachel Cummings, et al. Advances and open problems in federated learning. *Foundations and Trends® in Machine Learning*, 14(1–2):1–210, 2021.
- [2] Tian Li, Anit Kumar Sahu, Manzil Zaheer, Maziar Sanjabi, Ameet Talwalkar, and Virginia Smith. Federated optimization in heterogeneous networks. *Proceedings of Machine learning and systems*, 2:429–450, 2020.
- [3] Viraaji Mothukuri, Reza M Parizi, Seyedamin Pouriyeh, Yan Huang, Ali Dehghantanha, and Gautam Srivastava. A survey on security and privacy of federated learning. *Future Generation Computer Systems*, 115:619–640, 2021.
- [4] Brendan McMahan, Eider Moore, Daniel Ramage, Seth Hampson, and Blaise Aguera y Arcas. Communication-efficient learning of deep networks from decentralized data. In *Artificial intelligence and statistics*, pages 1273–1282. PMLR, 2017.
- [5] Yue Tan, Guodong Long, Jie Ma, Lu Liu, Tianyi Zhou, and Jing Jiang. Federated learning from pre-trained models: A contrastive learning approach. *arXiv preprint arXiv:2209.10083*, 2022.
- [6] Yue Tan, Guodong Long, Lu Liu, Tianyi Zhou, Qinghua Lu, Jing Jiang, and Chengqi Zhang. Fedproto: Federated prototype learning across heterogeneous clients. In *Proceedings of the AAAI Conference on Artificial Intelligence*, volume 36, pages 8432–8440, 2022.
- [7] Krishna Pillutla, Kshitiz Malik, Abdel-Rahman Mohamed, Mike Rabbat, Maziar Sanjabi, and Lin Xiao. Federated learning with partial model personalization. In *International Conference on Machine Learning*, pages 17716–17758. PMLR, 2022.
- [8] Avishek Ghosh, Jichan Chung, Dong Yin, and Kannan Ramchandran. An efficient framework for clustered federated learning. *Advances in Neural Information Processing Systems*, 33:19586–19597, 2020.
- [9] Tianfei Zhou and Ender Konukoglu. Fedfa: Federated feature augmentation. *arXiv preprint arXiv:2301.12995*, 2023.
- [10] Fengwen Chen, Guodong Long, Zonghan Wu, Tianyi Zhou, and Jing Jiang. Personalized federated learning with graph. *arXiv preprint arXiv:2203.00829*, 2022.
- [11] Jianyu Wang, Qinghua Liu, Hao Liang, Gauri Joshi, and H Vincent Poor. Tackling the objective inconsistency problem in heterogeneous federated optimization. *Advances in neural information processing systems*, 33:7611–7623, 2020.
- [12] Yue Wu, Shuaicheng Zhang, Wenchao Yu, Yanchi Liu, Quanquan Gu, Dawei Zhou, Haifeng Chen, and Wei Cheng. Personalized federated learning under mixture of distributions. *arXiv preprint arXiv:2305.01068*, 2023.
- [13] Yao Zhou, Jun Wu, Haixun Wang, and Jingrui He. Adversarial robustness through bias variance decomposition: A new perspective for federated learning. In Mohammad Al Hasan and Li Xiong, editors, *Proceedings of the 31st ACM International Conference on Information & Knowledge Management, Atlanta, GA, USA, October 17-21, 2022*, pages 2753–2762. ACM, 2022.
- [14] Liwei Che, Jiaqi Wang, Yao Zhou, and Fenglong Ma. Multimodal federated learning: A survey. *Sensors*, 23(15):6986, 2023.
- [15] Jiaqi Wang and Fenglong Ma. Federated learning for rare disease detection: a survey. *Rare Disease and Orphan Drugs Journal*, 2(22), 2023.
- [16] Chuhan Wu, Fangzhao Wu, Lingjuan Lyu, Yongfeng Huang, and Xing Xie. Communication-efficient federated learning via knowledge distillation. *Nature communications*, 13(1):2032, 2022.
- [17] Daliang Li and Junpu Wang. Fedmd: Heterogenous federated learning via model distillation. *arXiv preprint arXiv:1910.03581*, 2019.

- [18] Wenke Huang, Mang Ye, and Bo Du. Learn from others and be yourself in heterogeneous federated learning. In *Proceedings of the IEEE/CVF Conference on Computer Vision and Pattern Recognition*, pages 10143–10153, 2022.
- [19] Tao Lin, Lingjing Kong, Sebastian U Stich, and Martin Jaggi. Ensemble distillation for robust model fusion in federated learning. *Advances in Neural Information Processing Systems*, 33:2351–2363, 2020.
- [20] Sixing Yu, Wei Qian, and Ali Jannesari. Resource-aware federated learning using knowledge extraction and multi-model fusion. *arXiv preprint arXiv:2208.07978*, 2022.
- [21] Lichao Sun and Lingjuan Lyu. Federated model distillation with noise-free differential privacy. *arXiv preprint arXiv:2009.05537*, 2020.
- [22] Liping Yi, Gang Wang, Xiaoguang Liu, Zhuan Shi, and Han Yu. Fedgh: Heterogeneous federated learning with generalized global header. *arXiv preprint arXiv:2303.13137*, 2023.
- [23] Lingjuan Lyu, Han Yu, Xingjun Ma, Chen Chen, Lichao Sun, Jun Zhao, Qiang Yang, and S Yu Philip. Privacy and robustness in federated learning: Attacks and defenses. *IEEE transactions on neural networks and learning systems*, 2022.
- [24] Jiaqi Wang, Shenglai Zeng, Zewei Long, Yaqing Wang, Houping Xiao, and Fenglong Ma. Knowledge-enhanced semi-supervised federated learning for aggregating heterogeneous lightweight clients in iot. In *Proceedings of the 2023 SIAM International Conference on Data Mining (SDM)*, pages 496–504. SIAM, 2023.
- [25] Xingyi Yang, Daquan Zhou, Songhua Liu, Jingwen Ye, and Xinchao Wang. Deep model reassembly. *Advances in neural information processing systems*, 35:25739–25753, 2022.
- [26] Alireza Fallah, Aryan Mokhtari, and Asuman Ozdaglar. Personalized federated learning with theoretical guarantees: A model-agnostic meta-learning approach. *Advances in Neural Information Processing Systems*, 33:3557–3568, 2020.
- [27] Canh T Dinh, Nguyen Tran, and Josh Nguyen. Personalized federated learning with moreau envelopes. *Advances in Neural Information Processing Systems*, 33:21394–21405, 2020.
- [28] Xu Zhang, Yinchuan Li, Wenpeng Li, Kaiyang Guo, and Yunfeng Shao. Personalized federated learning via variational bayesian inference. In *International Conference on Machine Learning*, pages 26293–26310. PMLR, 2022.
- [29] Enmao Diao, Jie Ding, and Vahid Tarokh. Heterofl: Computation and communication efficient federated learning for heterogeneous clients. *arXiv preprint arXiv:2010.01264*, 2020.
- [30] Xiaofeng Lu, Yuying Liao, Chao Liu, Pietro Lio, and Pan Hui. Heterogeneous model fusion federated learning mechanism based on model mapping. *IEEE Internet of Things Journal*, 9(8):6058–6068, 2021.
- [31] Jiankai Sun, Xin Yang, Yuanshun Yao, Aonan Zhang, Weihao Gao, Junyuan Xie, and Chong Wang. Vertical federated learning without revealing intersection membership. *arXiv preprint arXiv:2106.05508*, 2021.
- [32] Yamini Bansal, Preetum Nakkiran, and Boaz Barak. Revisiting model stitching to compare neural representations. *Advances in neural information processing systems*, 34:225–236, 2021.
- [33] Samuel K Ainsworth, Jonathan Hayase, and Siddhartha Srinivasa. Git re-basin: Merging models modulo permutation symmetries. *arXiv preprint arXiv:2209.04836*, 2022.
- [34] Zizheng Pan, Jianfei Cai, and Bohan Zhuang. Stitchable neural networks. *arXiv preprint arXiv:2302.06586*, 2023.
- [35] Dang Nguyen, Trang Nguyen, Khai Nguyen, Dinh Phung, Hung Bui, and Nhat Ho. On cross-layer alignment for model fusion of heterogeneous neural networks. In *ICASSP 2023-2023 IEEE International Conference on Acoustics, Speech and Signal Processing (ICASSP)*, pages 1–5. IEEE, 2023.

- [36] Xingyi Yang, Jingwen Ye, and Xinchao Wang. Factorizing knowledge in neural networks. In *European Conference on Computer Vision*, pages 73–91. Springer, 2022.
- [37] Simon Kornblith, Mohammad Norouzi, Honglak Lee, and Geoffrey Hinton. Similarity of neural network representations revisited. In *International Conference on Machine Learning*, pages 3519–3529. PMLR, 2019.
- [38] Ting Chen, Simon Kornblith, Mohammad Norouzi, and Geoffrey Hinton. A simple framework for contrastive learning of visual representations. In *International conference on machine learning*, pages 1597–1607. PMLR, 2020.
- [39] Ying Zhang, Tao Xiang, Timothy M Hospedales, and Huchuan Lu. Deep mutual learning. In *Proceedings of the IEEE conference on computer vision and pattern recognition*, pages 4320–4328, 2018.

Towards Personalized Federated Learning via Heterogeneous Model Reassembly (Appendix)

1 Pseudo-code of pFedHR

Algorithm 1 shows the pseudo-code of the proposed pFedHR model, which contains two main updates: the server update (lines 3-11) and the client update (lines 12 - 17). The details of reassembly candidate generation can be found in the main manuscript (Algorithm 1 on Page 5).

Algorithm 1: Algorithm Flow of pFedHR.

Input: Local data $\mathcal{D}_1, \mathcal{D}_2, \dots, \mathcal{D}_N$, the number of active clients B , communication rounds T , the number of local training epochs E_c , the number of fine-tuning epochs at the server E_s , cluster number K .

```
1 for each communication round  $t = 1, 2, \dots, T$  do
2   Randomly sample  $B$  active clients and their model parameters are denoted as
    $\{\mathbf{w}_t^1, \mathbf{w}_t^2, \dots, \mathbf{w}_t^B\}$ ;
3   Server Update
4     for each  $n \in [1, \dots, B]$  do
5       Conduct layer-wise ecomposition on  $\mathbf{w}_t^n = [(\mathbf{L}_{t,1}^n, O_1^n), \dots, (\mathbf{L}_{t,H}^n, O_E^n)]$ ;
6     end
7     Conduct function-driven layer grouping with Eq. (4) to obtain  $\{\mathcal{G}_t^1, \mathcal{G}_t^2, \dots, \mathcal{G}_t^K\}$ ;
8     Conduct reassembly candidate generation to obtain  $\{\mathbf{c}_t^1, \dots, \mathbf{c}_t^M\}$  following
      $\mathcal{R}_1, \mathcal{R}_2, \mathcal{R}_3$ , and  $\mathcal{R}_4$ ;
9     Conduct layer stitching on the generated candidates;
10    Conduct similarity calculation on pairs of models with Eq. (5);
11    Distribute the personalized models back to the clients accordingly.
12   Client Update
13     for each  $n \in [1, \dots, B]$  do
14       for each local epoch  $e$  from 1 to  $E_c$  do
15         Update  $\mathbf{w}_t^n$  with Eq. (6);
16       end
17     end
18   Upload  $B$  models  $\{\mathbf{w}_t^1, \mathbf{w}_t^2, \dots, \mathbf{w}_t^B\}$  back to the server;
19 end
```

2 Implementation Details

The proposed pFedHR is implemented in Pytorch 2.0.1 and runs on NVIDIA A100 with CUDA version 12.0 on a Ubuntu 20.04.6 LTS server. The hyperparameter λ in Eq. (6) is 0.2. We use Adam as the optimizer. The learning rate of the local client learning and the server fine-tuning learning rate are both equal to 0.001.

2.1 Model Details

In our experiments, we have 4 CNN models with different complexity. The details are shown as follows. In each convolutional NN sequential block, there are 1 convolutional layer, a max pooling layer, and a ReLU function.

M1: $Cov1:\{Conv2d (kernel\ size = 5) \rightarrow ReLU \rightarrow MaxPool2D (kernel\ size = 2, stride = 2)\} \rightarrow Cov2:\{Conv2d (kernel\ size = 5) \rightarrow ReLU \rightarrow MaxPool2D (kernel\ size = 2, stride = 2)\} \rightarrow FC1:\{Linear \rightarrow ReLU\} \rightarrow Dropout \rightarrow FC2:Linear.$

M2: $Cov1:\{Conv2d (kernel\ size = 5) \rightarrow ReLU \rightarrow MaxPool2D (kernel\ size = 2, stride = 2)\} \rightarrow Cov2:\{Conv2d (kernel\ size = 5) \rightarrow ReLU \rightarrow MaxPool2D (kernel\ size = 2, stride = 2)\} \rightarrow Cov3:\{Conv2d (kernel\ size = 5) \rightarrow ReLU\} \rightarrow FC1:\{Linear \rightarrow ReLU\} \rightarrow Dropout \rightarrow FC2:Linear.$

M3: $Cov1:\{Conv2d (kernel\ size = 5) \rightarrow ReLU \rightarrow MaxPool2D (kernel\ size = 2, stride = 2)\} \rightarrow Cov2:\{Conv2d (kernel\ size = 5) \rightarrow ReLU \rightarrow MaxPool2D (kernel\ size = 2, stride = 2)\} \rightarrow Cov3:\{Conv2d (kernel\ size = 5) \rightarrow ReLU\} \rightarrow Cov4:\{Conv2d (kernel\ size = 5) \rightarrow ReLU \rightarrow MaxPool2D (kernel\ size = 2, stride = 2)\} \rightarrow Cov5:\{Conv2d (kernel\ size = 5) \rightarrow ReLU\} \rightarrow FC1:\{Linear \rightarrow ReLU \rightarrow Dropout\} \rightarrow FC2:\{Linear \rightarrow ReLU\} \rightarrow FC3:\{Linear \rightarrow ReLU\} \rightarrow FC4:Linear.$

M4: $Cov1:\{Conv2d (kernel\ size = 5) \rightarrow BatchNorm2d \rightarrow ReLU\} \rightarrow Cov2:\{Conv2d (kernel\ size = 3) \rightarrow ReLU \rightarrow MaxPool2D (kernel\ size = 2, stride = 2)\} \rightarrow Cov3:\{Conv2d (kernel\ size = 3) \rightarrow BatchNorm2d \rightarrow ReLU\} \rightarrow Cov4:\{Conv2d (kernel\ size = 5) \rightarrow ReLU \rightarrow MaxPool2D (kernel\ size = 2, stride = 2) \rightarrow Dropout\} \rightarrow Cov5:\{Conv2d (kernel\ size = 3) \rightarrow BatchNorm2d \rightarrow ReLU\} \rightarrow Cov6:\{Conv2d (kernel\ size = 3) \rightarrow ReLU \rightarrow MaxPool2D (kernel\ size = 2, stride = 2)\} \rightarrow FC1:\{Linear \rightarrow ReLU \rightarrow Dropout\} \rightarrow FC2:\{Linear \rightarrow ReLU\} \rightarrow FC3:\{Linear \rightarrow ReLU\} \rightarrow FC4:Linear.$

2.2 Details of Rule \mathcal{R}_2 (Operation Order)

We introduce the rule \mathcal{R}_2 (operation order) in Line 11 of the algorithm in the main manuscript. We follow existing work [1, 2, 3, 4, 5] to define the following rules:

1. A CNN typically has convolutional layers, pooling layers, and fully connected layers, which requires the generated candidate to have these functional layers.
2. The typical operation order is convolution layers \rightarrow ReLU layers \rightarrow pooling layers \rightarrow fully connected layers.

2.3 Public Data Sensitivity Analysis

2.3.1 Experiment Results of Public Data Sensitivity on SVHN with 100 Clients

Figure 1 shows the experimental results with 100 clients. The clients hold the SVHN data, and we alternatively change the (labeled and unlabeled) public data and report the results for both IID and Non-IID settings. We can observe the same results as those on the 12 clients (Figure 1 in the main manuscript). All approaches can achieve the best performance when using SVNH as the public data. Although using other public data, the performance of all approaches drops, the performance change of the proposed $pFedHR$ is lowest. Besides, even using other public data, $pFedHR$ can achieve comparable or better performance to baselines. For example, in Figure 1(b), when $pFedHR$ uses the MNIST as the public data, its performance is comparable to FedMD and better than FedGH using SVHN as the public data. These results confirm that the proposed $pFedHR$ can handle the public data sensitivity issue.

2.3.2 Experiment Results of Public Data Sensitivity on CIFAR-10 with 12 Clients

We also validate the public data sensitivity on CIFAR-10, where clients hold data from CIFAR-10, and we alternatively change the public data. The results are shown in Figures 2 and 3. We have the same observations as we discussed before. Using public data with different distributions makes the performance drop, but the proposed $pFedHR$ has the smallest drop ratio.

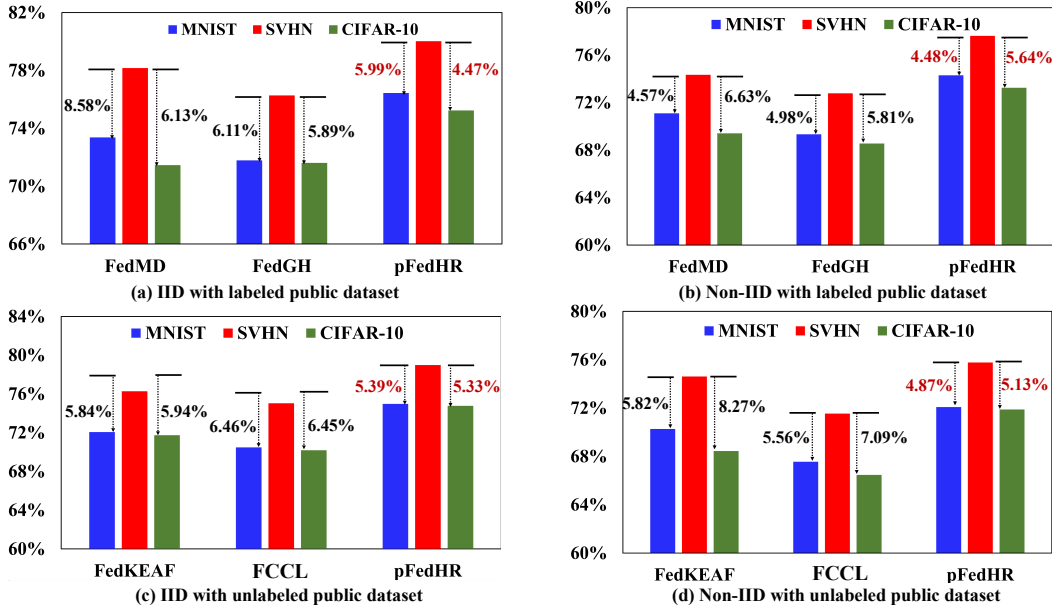


Figure 1: Results with 100 clients.

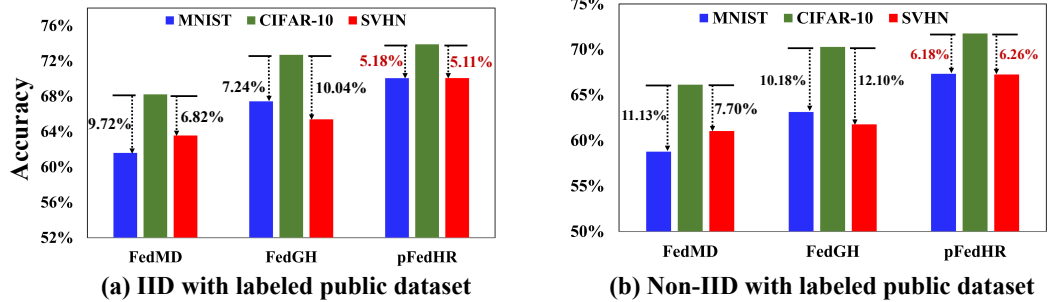


Figure 2: Results with CIFAR-10 private dataset and labeled public datasets.

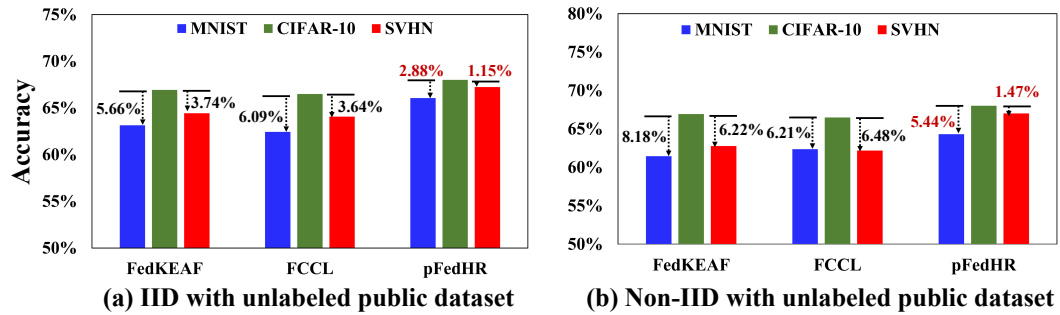


Figure 3: Results with CIFAR-10 private dataset and unlabeled public datasets.

3 Limitation

All the experimental results demonstrate the effectiveness of the proposed pFedHR. However, pFedHR still have the following limitations:

1. In our experiments, we use four different CNN-based models and randomly send them to clients. The reason for using these simple models is that they can save computational resources. In our model design, we will calculate the CKA score between any pair of layers.

In other words, if the local model is very deep (with multiple layers), the computational complexity will be very high.

2. In real-world applications, the client models may be more complicated. To deploy the proposed pFedHR in a real environment, we need to slightly modify the layer-wise decomposition and use block-wise decomposition as [6] and redefine the rules used for generating candidates accordingly.
3. In our experiments, we only test the designed model on the image datasets. In real-world applications, multiple types of data may be stored in each client. How to handle other types of data with heterogeneous model reassembly is one of our major future works.

4 Broader Impacts

The proposed pFedHR addresses the practical challenge of model heterogeneity in federated learning. By introducing heterogeneous model reassembly and personalized federated learning, this research contributes to the advancement of federated learning techniques, potentially improving the efficiency and effectiveness of collaborative machine learning in distributed systems.

The pFedHR framework automatically generates informative and diverse personalized candidates with minimal human intervention. This has the potential to reduce the burden on human experts and practitioners, making the process of model personalization more efficient and scalable. It opens up possibilities for deploying federated learning systems in real-world scenarios where manual customization is impractical or time-consuming.

The proposed heterogeneous model reassembly technique in pFedHR tries to mitigate the adverse impact caused by using public data with different distributions from the client data. This can be beneficial in scenarios where privacy concerns limit the availability of extensive client data, such as healthcare, enabling the utilization of publicly available data while maintaining a certain level of model performance. It promotes the ethical and responsible use of data and encourages collaboration between organizations and researchers in a privacy-preserving manner.

References

- [1] Alex Krizhevsky, Ilya Sutskever, and Geoffrey E Hinton. Imagenet classification with deep convolutional neural networks. *Communications of the ACM*, 60(6):84–90, 2017.
- [2] Karen Simonyan and Andrew Zisserman. Very deep convolutional networks for large-scale image recognition. *arXiv preprint arXiv:1409.1556*, 2014.
- [3] Kaiming He, Xiangyu Zhang, Shaoqing Ren, and Jian Sun. Deep residual learning for image recognition. In *Proceedings of the IEEE conference on computer vision and pattern recognition*, pages 770–778, 2016.
- [4] Christian Szegedy, Wei Liu, Yangqing Jia, Pierre Sermanet, Scott Reed, Dragomir Anguelov, Dumitru Erhan, Vincent Vanhoucke, and Andrew Rabinovich. Going deeper with convolutions. In *Proceedings of the IEEE conference on computer vision and pattern recognition*, pages 1–9, 2015.
- [5] Gao Huang, Zhuang Liu, Laurens Van Der Maaten, and Kilian Q Weinberger. Densely connected convolutional networks. In *Proceedings of the IEEE conference on computer vision and pattern recognition*, pages 4700–4708, 2017.
- [6] Xingyi Yang, Daquan Zhou, Songhua Liu, Jingwen Ye, and Xinchao Wang. Deep model reassembly. *Advances in neural information processing systems*, 35:25739–25753, 2022.